



## Thermoluminescence of UV-irradiated $\alpha$ - $\text{Al}_2\text{O}_3\text{:C,Mg}$

N.M. Trindade<sup>a,b,\*\*</sup>, M.G. Magalhães<sup>a</sup>, M.C.S. Nunes<sup>a</sup>, E.M. Yoshimura<sup>b</sup>, L.G. Jacobsohn<sup>c</sup>

<sup>a</sup> Department of Physics, Federal Institute of Education, Science and Technology of São Paulo, São Paulo, SP, Brazil

<sup>b</sup> Institute of Physics, University of São Paulo - USP, São Paulo, SP, Brazil

<sup>c</sup> Department of Materials Science and Engineering, Clemson University, Clemson, SC, USA

### ARTICLE INFO

#### Keywords:

$\text{Al}_2\text{O}_3\text{:C,Mg}$   
UV irradiation  
Beta irradiation  
Thermoluminescence  
Color centers

### ABSTRACT

The effects of ultraviolet (UV) radiation exposure on the thermoluminescence (TL) of aluminium oxide co-doped with carbon and magnesium ( $\text{Al}_2\text{O}_3\text{:C,Mg}$ ) are reported. An  $\text{Al}_2\text{O}_3\text{:C,Mg}$  single crystal was investigated as a potential UV TL dosimeter after exposure to a Hg lamp radiation. The TL peak intensity and area under the curve signals were investigated as a function of the UV exposure time. Intense TL signal was obtained after UV radiation, and the area of the main TL peak at 456 K exponentially increasing with UV exposure time (within 10–120 s), with a trend for saturation for long irradiation times. These results were interpreted against similar measurements using beta radiation, showing that the same defects are involved in the TL response for both types of radiation, while the different irradiation response to the two types of radiation was related to the differences in the energy dissipation characteristics, and how they affect the concentration of F-type/F-aggregate centers.

### 1. Introduction

Ultraviolet (UV) radiation corresponds to a narrow fraction of the electromagnetic spectrum and is divided in three spectral regions: UVA (315–400 nm), UVB (280–315 nm) and UVC (100–280 nm) [1]. The increasing use of UV radiation from artificial sources such as cosmetic tanning beds, welding machines and xenon arcs, and a variety of lamps for medical therapy can significantly contribute to the risks of UV overexposure [2], possibly leading to skin cancer, erythema, and inflammation of the eyes [3]. Within this context, measurement methods and new sensors for assessing UV exposure have become increasingly important.

Thermoluminescence (TL) corresponds to the light emission upon heating of insulating or semiconducting materials previously exposed to ionizing radiation that is not incandescence [4]. UV dosimetry can be executed through TL measurements using carbon-doped aluminum oxide ( $\text{Al}_2\text{O}_3\text{:C}$ ) [5–10], and some authors have shown that  $\text{Al}_2\text{O}_3\text{:C}$  exhibits intense TL response after UV irradiation [7,9,10]. More recently, Yukihara et al. investigated the effects of deep trap filling using UV-irradiated  $\text{Al}_2\text{O}_3\text{:C}$  samples [11], while Pagonis et al. [12] carried out a quantitative kinetic model that described the TL response of UV irradiated  $\text{Al}_2\text{O}_3\text{:C}$  that was later verified experimentally by Gronchi and Caldas [13].

$\text{Al}_2\text{O}_3\text{:C}$  is well-known as a high sensitivity dosimeter for personal

and environmental ionizing radiation dosimetry [14,15]. The high sensitivity of this material is due to the C doping of  $\text{Al}_2\text{O}_3$  that promotes the formation of a large concentrations of F and  $\text{F}^+$  centers [16]. Consequently, this has motivated the investigation of  $\text{Al}_2\text{O}_3\text{:C}$  crystals with other dopants besides carbon. For example,  $\text{Al}_2\text{O}_3\text{:C,Mg}$ , introduced by Akselrod et al. [17], is a luminescent material with application in imaging and possibly in optical data storage [18,19]. As in the case of  $\text{Al}_2\text{O}_3\text{:C}$ , besides the high concentrations of F and  $\text{F}^+$  centers,  $\text{Al}_2\text{O}_3\text{:C,Mg}$  also contains aggregates of these centers such as  $\text{F}_2$ ,  $\text{F}_2^+$ , and  $\text{F}_2^{2+}$ . However, it also contains oxygen vacancies charge compensated by Mg, i.e.,  $\text{F}^+$  (Mg) centers and their aggregates such as  $\text{F}_2^+$ (Mg),  $\text{F}_2^+$ (2 Mg) and  $\text{F}_2^{2+}$ (2 Mg) [16,20,21].  $\text{Al}_2\text{O}_3\text{:C,Mg}$  has been successfully evaluated for the dosimetry of neutrons, protons and heavy charged particles [22–24]. Currently, it is used as a fluorescent nuclear track detector (FNTD) [22] when laser-induced fluorescence allows for fast non-destructive three dimensional mapping using confocal scanning microscopy [22,25]. Therefore, images can be automatically obtained wherein radiation tracks appear in the form of bright spots on a dark background, allowing for track counting with image processing software [26,27].

$\text{Al}_2\text{O}_3\text{:C,Mg}$  has also been investigated for TL applications [14,16,28,29], and while it is promising for the monitoring of beta, gamma and X-ray radiation dosimetry [18,21,30,31], there have been no previous works targeted at the UV-induced TL of this material. In this context, the

\* Corresponding author.

E-mail address: [ntrindade@ifsp.edu.br](mailto:ntrindade@ifsp.edu.br) (N.M. Trindade).

<https://doi.org/10.1016/j.jlumin.2020.117195>

Received 4 November 2019; Received in revised form 10 February 2020; Accepted 4 March 2020

Available online 5 March 2020

0022-2313/© 2020 Elsevier B.V. All rights reserved.

objective of this paper is to investigate the TL response an  $\text{Al}_2\text{O}_3:\text{C,Mg}$  single crystal irradiated by artificial UV light source, and toward the understanding of the effects of different types of radiation on the TL response of this material.

## 2. Materials and methods

The sample investigated was an  $\text{Al}_2\text{O}_3:\text{C,Mg}$  single crystal grown by the Czochralski technique by Landauer, Inc., Crystal Growth Division, Stillwater, OK, USA. The single crystal was cut into a rectangular parallelepiped (8 mm long, 1.6 mm wide and 0.5 mm thick) with one polished side, and mass of 48 mg.

Optical absorption measurements were carried out in the range from 200 to 700 nm using a Shimadzu 3600 series UV-Vis spectrophotometer.

TL measurements were carried out using a commercial automated TL/OSL reader made by Risø National Laboratory (model DA-20). TL glow curves were obtained after exposure to UV and/or beta irradiation for up to 120 s, using a heating rate of 1 K/s, from room temperature (RT) to 675 K. The TL signal was detected with a bi-alkali photomultiplier tube behind an UV-transmitting glass filter (Hoya U-340, 7.5 mm thick), and a mask with 5 mm dia. pinhole. Irradiation was executed at RT using the built-in  $^{90}\text{Sr}/^{90}\text{Y}$  beta source of the TL/OSL reader (activity = 1.48 GBq May/2010; dose rate = 10 mGy/s). All measurements were carried out in nitrogen atmosphere to prevent spurious signals.

UV exposure was executed with a 1000 W Oriel mercury arc lamp, with irradiance of  $5.4 \text{ W/m}^2$  at the sample position, measured with a Delta OHM radiometer model DO 9721 coupled to a LP 9021 UVA sensor. UV exposure was executed with different time intervals, from 10 to 120 s, with the sample being placed directly under the lamp at a distance of 1 m. The lamp spectrum was obtained with an Ocean Optics QE65 Pro Scientific-grade spectrometer in the same position as the sample. The mercury lamp spectral emission includes the visible/near infrared (400–1000 nm; 94.6%) and UV (200–400 nm; 5.4%) regions of the electromagnetic spectrum with the relative intensities of the UV spectral regions being 58% UVA, and 14% UVB, and 28% UVC.

TL glow curve analysis used the GlowFit software [32] that is based on the first-order kinetics model by Randall-Wilkins [33]. The TL results were analyzed in terms of the area under the curve, the activation energy  $E$ , and the TL peak positions. Since all measurements were carried out with the same sample, results were not normalized by the sample mass.

## 3. Results

A typical optical absorption spectrum in the UV-visible spectral range is shown in Fig. 1. As shown in Ref. [19,21,34] a variety of defect absorption bands are present in  $\text{Al}_2\text{O}_3:\text{C,Mg}$  due to crystal growth in a highly reducing atmosphere and the presence of aliovalent magnesium and carbon impurities.

Fig. 2 shows the TL glow curves of  $\text{Al}_2\text{O}_3:\text{C,Mg}$  single crystal obtained after different UV irradiation times from 10 to 120 s, while the inset shows the same results in semi-logarithmic scale to highlight the contribution of the low-temperature peaks within RT to 400 K. Fig. 3 shows a comparison between the TL glow curves obtained for the same sample after beta (black line) and UV (red line) radiation, respectively.

Fig. 4 shows the result of the best fit using the GlowFit software (best fit: continuous red lines) of the main TL peak of the experimental glow curves (open black circle) obtained after 60s of UV exposure time. Similar results were obtained for the other glow curves, with best fittings achieving a figure of merit (FOM) below 5%, demonstrating the good quality of the fittings.

Fig. 5 shows the behavior of the integral of the main TL obtained with GlowFit as a function of the UV (open black circles) and beta radiation (open black squares) exposure time. In the case of UV irradiation, the error bars represent the standard deviation of the three experimental runs. Fig. 6 shows the effects of ten sequential TL

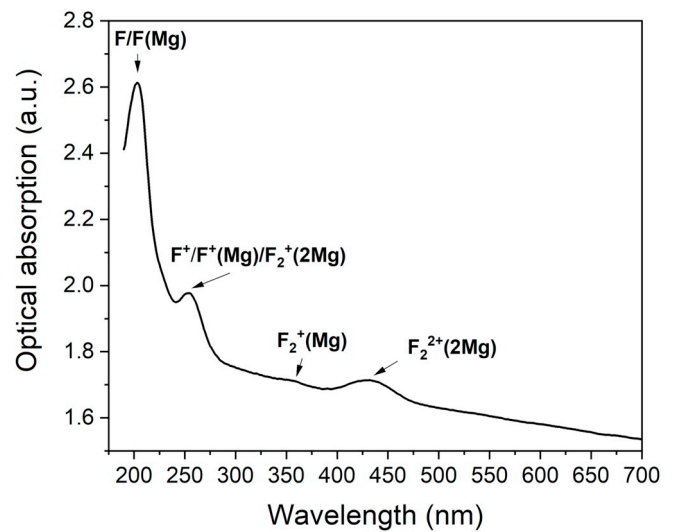


Fig. 1. Optical absorption of a  $\alpha\text{-Al}_2\text{O}_3:\text{C,Mg}$  single crystal.

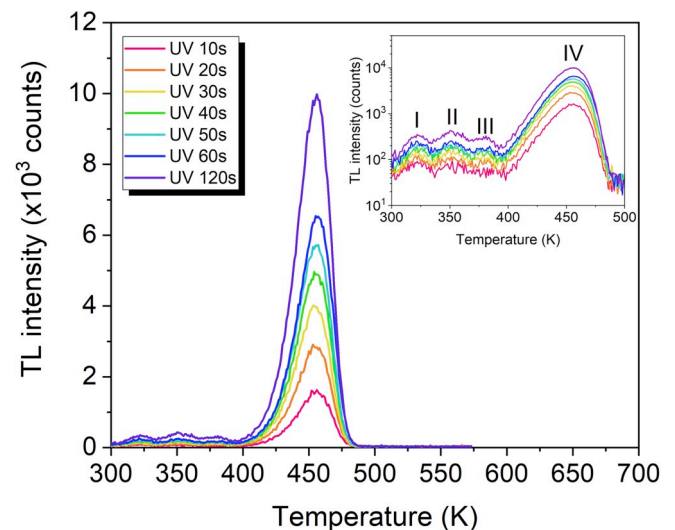


Fig. 2. TL glow curves of  $\text{Al}_2\text{O}_3:\text{C,Mg}$  single crystal obtained at 1 K/s heating rate as function of different UV exposure times. The inset shows the same TL glow curves in semi-log scale.

measurements after individual UV (30s – open black circles) and beta (10s – open black squares) irradiations.

## 4. Discussion

The optical absorption spectrum, Fig. 1, was dominated by broad absorption bands centered at about 205 and 255 nm, together with bands at about 355 and 435 nm, on top of a background due to light scattering by the unpolished surface. Based on previous works [21,35,36], the band centered at 205 nm was assigned to F and F(Mg) centers, at 255 nm to  $\text{F}^+$ ,  $\text{F}^+(\text{Mg})$  and  $\text{F}_2^+(2\text{Mg})$  centers, at 355 nm to  $\text{F}_2^+(\text{Mg})$  centers, and the band at about 435 nm to  $\text{F}_2^{2+}(2\text{Mg})$ . According to Ref. [11], UV irradiation causes ionization of F centers by the mechanism  $F + h\nu \rightarrow F^+ + e^-$  creating a free electron and increasing the concentration of  $\text{F}^+$  centers at the expense of F centers. This phenomenon is expected to have great influence on the TL response of  $\text{Al}_2\text{O}_3:\text{C,Mg}$ . It is noted that defect-free  $\text{Al}_2\text{O}_3$  is transparent in the UVA and UVB spectral regions, and only weakly absorbing in the UVC region [37]. It is the presence of the F-type and F-aggregate defects that cause the strong absorption needed for UV dosimetry. Moreover, if corrected for the

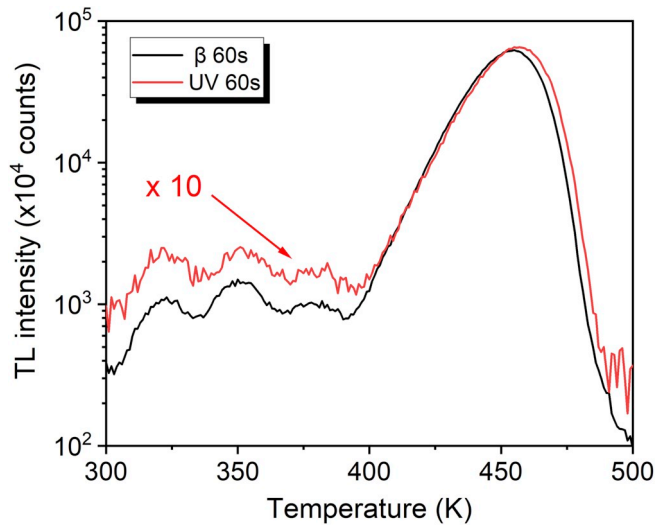


Fig. 3. TL glow curves in semi-log scale of  $\text{Al}_2\text{O}_3:\text{C,Mg}$  single crystal obtained under beta (black line) and UV (red line) radiation.

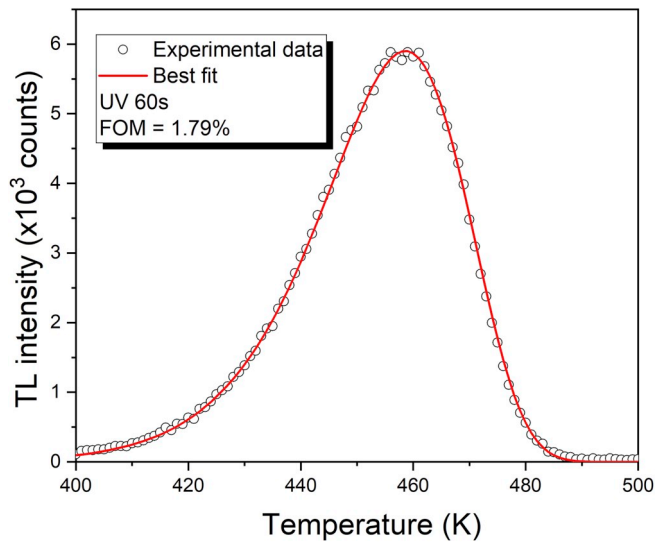


Fig. 4. TL glow curve (open black circles) of  $\text{Al}_2\text{O}_3:\text{C,Mg}$  single crystal together with best fit (red line) obtained at 60s UV exposure time.

scattering background, these results show that UVA (315–400 nm) and UVB (280–315 nm) were barely absorbed by the sample, while strong absorption occurred within the UVC region (100–280 nm) by  $\text{F}^-$ ,  $\text{F}^+(\text{Mg})$  and  $\text{F}_2^+(2\text{Mg})$  centers.

The UV TL glow curves of  $\text{Al}_2\text{O}_3:\text{C,Mg}$  single crystal (Fig. 2) revealed three low intensity peaks at temperatures at about 320 (peak I), 350 (peak II), and 375 K (peak III), in addition to the main peak at 456 K (peak IV). No TL signal was observed above 500 K. It was also possible to observe in Fig. 2 an increase in the intensity of the main TL glow peak for increasing UV exposures. On the other hand, the behavior of the low-temperature peaks with UV exposure time was not so well defined.

In Fig. 3, the comparison between the sample exposed to UV and beta radiation showed similar glow curves. According to the literature [21, 31,38], the main TL peak of beta irradiated  $\text{Al}_2\text{O}_3:\text{C,Mg}$  single crystal is the result of emissions at 325, 415, 520 and 750 nm likely corresponding to  $\text{F}^+$ ,  $\text{F}$ ,  $\text{F}_2^+(2\text{Mg})$  and  $\text{F}_2^+(2\text{Mg})$  centers, respectively, depending on the temperature [21]. These results showed that the TL response of  $\text{Al}_2\text{O}_3:\text{C,Mg}$  to be the same after UV and beta irradiation.

According to Yukihiro et al. [11], the TL behavior of  $\text{Al}_2\text{O}_3:\text{C}$  can be

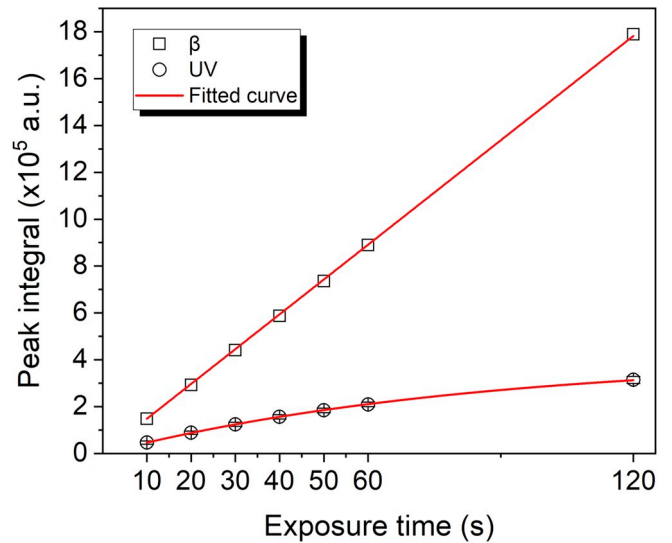


Fig. 5. Integrated intensity (area) of main peak from TL glow curves of  $\text{Al}_2\text{O}_3:\text{C,Mg}$  single crystal as a function of the beta (open black squares) and UV (open black circles) exposure time together with best fittings (red line).

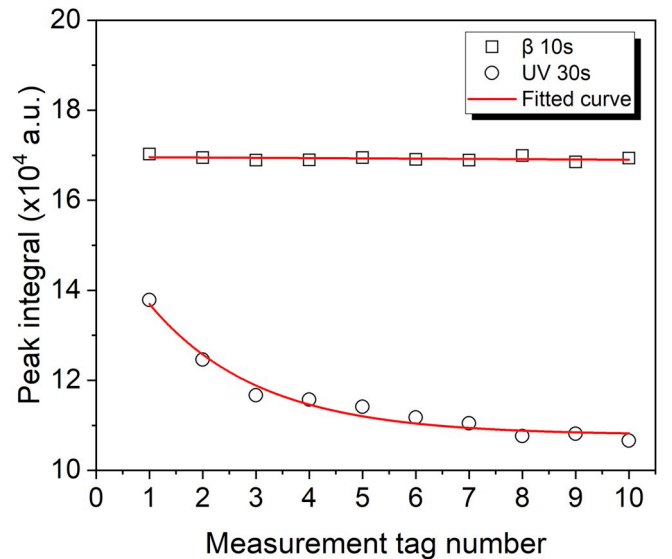


Fig. 6. Integrated intensity (area) of main TL peak from ten sequential TL measurements as a function of the beta (open black squares) and UV (open black circles) exposure time together with best fittings (red line).

explained by taking into account the main dosimetric trap (MDT), the deep electron trap (DET), and the deep hole trap (DHT), altogether with  $\text{F}$  and  $\text{F}^+$  centers. Irradiation creates electron-hole pairs, wherein electrons are either trapped at the MDT or recombine with existing  $\text{F}^+$  centers, creating  $\text{F}$  centers, and free holes are captured by the  $\text{F}$  centers, increasing the concentration of  $\text{F}^+$  centers.

Previous reports on  $\text{Al}_2\text{O}_3:\text{C,Mg}$  irradiated with ionizing radiation also showed that TL peaks I, II and IV (cf. Fig. 2) presented first-order kinetics [30,39]. On the other hand, the results for peak III are uncertain because of its weaker relative intensity combined with its proximity to peaks I and II and no clear conclusion on the kinetic order of its recombination mechanism could be drawn. Based on this, this work focused on the analysis of the main peak as a function of the UV exposure. Fig. 4 illustrates the fitting results of the main TL peak of the glow curve obtained after 60s of UV irradiation. The results of the GlowFit analysis of this peak for UV irradiation were  $T_m = (456.1 \pm 0.81)\text{K}$  and  $E$

$= (1.37 \pm 0.01)$  eV. In comparison, the values for beta irradiation were  $T_m = (455.3 \pm 0.07)$  K and  $E = (1.35 \pm 0.02)$  eV. The frequency factor was of the order of  $10^{14} \text{ s}^{-1}$  for both types of radiation. The  $E$  and  $s$  values were in agreement with values reported in previous works [30, 39]. Moreover, within the standard deviation, the peak position and the  $E$  value were independent of the UV exposure time, in agreement with the expected behavior related to a first-order kinetics recombination mechanism.

In Fig. 5, the integral of the main TL glow peak (from 400 to 500 K) under beta and UV irradiation is shown. For beta irradiation, a linear response with the exposure time was observed, in agreement with previous findings [14]. The linear best fit (red line;  $R^2 = 0.999$ , where  $R^2$  is the coefficient of determination) yielded the angular coefficient  $= (1.49 \pm 0.01) \times 10^4$  counts/s with the intercept fixed at the origin. On the other hand, for UV irradiation, a nearly linear relationship was found only for short UV exposure times, *i.e.*, less than about 30 s, with a trend for saturation for longer UV exposure times. The UV irradiation curve was best fitted with a function of the type:

$$I(t) = a(1 - e^{-bt})$$

That is a saturating exponential, where  $I(t)$  is the main TL peak integral,  $t$  is the UV exposure time in s,  $a$  is a proportionality constant, and  $b$  is the exponential factor. The values obtained with the best fit procedure (red line,  $R^2 = 0.999$ ) were  $a = (4.12 \pm 0.04) \times 10^5$  counts/s and  $b = (1.19 \pm 0.02) \times 10^{-2} \text{ s}^{-1}$ .

It is speculated that the different irradiation response of  $\text{Al}_2\text{O}_3\text{:C,Mg}$  to the two types of radiation could be related to the differences in the energy dissipation characteristics, and how they affect the concentration of F-type/F-aggregate centers, as discussed below. Beta radiation dissipates energy through the interaction with electrons and nuclei of the material. While the direct ionization of F-type/F-aggregate centers generating ionizing centers is possible, the yield of this mechanism is expected to be negligible given the concentration of these centers being much lower than the electron concentration of the material. Beta irradiation leads to the creation of a cascade of electron-hole pairs distributed in the material and previous investigation showed that essentially only one type of color center (the F center) is created due to electron irradiation of sapphire [40]. The fate of these charge carriers is very important as they can affect the concentration of the recombination centers associated with TL peak IV that, in a previous work, were determined to be F,  $\text{F}^+$ ,  $\text{F}^+(\text{Mg})$ ,  $\text{F}_2$ ,  $\text{F}_2^+(2 \text{ Mg})$ , and  $\text{F}_2^{2+}(2 \text{ Mg})$  centers [21]. Some of the electron-hole pairs created by beta radiation will recombine non-radiatively generating phonons (heat), while some of the free charge carriers will be captured by traps that later will be responsible for the TL signal upon heating. Further, some electron-hole pairs will recombine radiatively at the many different F-type/F-aggregate centers that have been observed in the sample (cf. Fig. 1) generating radioluminescence. While an ionized F-type/F-aggregate center can capture a free electron, the capture of a free electron by the  $\text{F}^+$ ,  $\text{F}^+(\text{Mg})$ , and  $\text{F}_2^+(2 \text{ Mg})$  centers is highlighted because transformation into a neutrally charged center, *i.e.*, F,  $\text{F}(\text{Mg})$ , and  $\text{F}_2(2 \text{ Mg})$ , respectively, will decrease the concentration of  $\text{F}^+$ ,  $\text{F}^+(\text{Mg})$ , and  $\text{F}_2^+(\text{Mg})$  centers that are some of the recombination centers in  $\text{Al}_2\text{O}_3\text{:C,Mg}$  detected in this work. Since these ionized centers are involved in the TL recombination process, the decrease of their concentration is expected to affect the TL signal intensity upon readout. It is noted, however, that TL measurements were performed in this work with a UV filter that allowed transmission within *ca.* 260 and 390 nm such that only the emission of  $\text{F}^+$  at 326 nm,  $\text{F}^+(\text{Mg})$  at 325 nm, and  $\text{F}_2^+(\text{Mg})$  at 385 nm, and partially of F and  $\text{F}(\text{Mg})$  centered at about 413 nm [21] were detected, *i.e.* only changes in the populations of these centers would be detected through TL readout.

In addition to these mechanisms, the presence of deep traps in  $\text{Al}_2\text{O}_3\text{:C,Mg}$  needs to be considered. While the presence of deep traps in  $\text{Al}_2\text{O}_3\text{:C,Mg}$  has not been experimentally confirmed, their presence in the very

similar material  $\text{Al}_2\text{O}_3\text{:C}$  is well-known [11,41] thus supporting the assumption that they are also present in  $\text{Al}_2\text{O}_3\text{:C,Mg}$ . If the concentration of deep electron traps is larger than that of the ionized F-type/F-aggregate centers, then the capture of free electrons by deep traps will dominate and the concentration of the ionized F-type/F-aggregate centers is not expected to change significantly. On the other hand, if the concentration of ionized F-type/F-aggregate centers is larger than that of deep electron traps, then an increase of the concentration of F-type/F-aggregate centers concomitant to a decrease of ionized F-type/F-aggregate centers is expected. A similar argument related to the concentration of deep hole traps can be stated, with a larger concentration of deep hole traps facilitating the capture of free electrons by ionized F-type/F-aggregate centers. Our results showed a linear increase of the integrated TL intensity of peak IV with exposure time to beta irradiation, thus suggesting that the concentration of the recombination centers possibly remained unchanged after irradiation within the limits of our experimental sensitivity.

UV photons, on the other hand, are only absorbed in  $\text{Al}_2\text{O}_3\text{:C,Mg}$  because of the presence of F-type and F-aggregate defects (defect-free  $\text{Al}_2\text{O}_3$  is transparent to UV [37]). Each UV photon may excite or ionize a F-type/F-aggregate defect, but when the UV photon excites a F-type/F-aggregate center, no free electrons are created. It is only when the UV photon ionizes a F-type/F-aggregate center that a free electron is created allowing for its trapping, and later TL signal upon heating. Consequently, the creation of free electrons requires F-type/F-aggregate centers to be ionized, thus reducing the population of these centers available for the next incoming UV photon and for TL recombination. Specifically, our results showed that only F,  $\text{F}(\text{Mg})$ ,  $\text{F}^+$ ,  $\text{F}^+(\text{Mg})$ , and  $\text{F}_2^+(2 \text{ Mg})$  centers were capable of effectively absorb UV radiation (Fig. 1). Among these centers, the ionization of  $\text{F}^+$ ,  $\text{F}^+(\text{Mg})$  and  $\text{F}_2^+(2 \text{ Mg})$  centers will render them ineffective for future UV absorption and for contributing to the TL peak IV recombination. Since our TL measurements were only sensitive to the emission of  $\text{F}^+$ ,  $\text{F}^+(\text{Mg})$ ,  $\text{F}_2^+(\text{Mg})$ , and partially of F and  $\text{F}(\text{Mg})$ , we hypothesize that the ionization of  $\text{F}^+$ ,  $\text{F}^+(\text{Mg})$ , and  $\text{F}_2^+(\text{Mg})$  centers leads to the progressive decrease of the TL signal for longer irradiation times. On this regard, Fig. 6 shows the progressive decrease of the TL main peak integral after ten consecutive TL readouts after 30 s long UV irradiations. The decrease was fitted with an exponential function, and was tentatively ascribed to the decrease of F-type/F-aggregate centers, specially all or some among  $\text{F}^+$ ,  $\text{F}^+(\text{Mg})$ , and  $\text{F}_2^+(\text{Mg})$ , as discussed above. This behavior is consistent with the trend for saturation of the TL main peak signal for longer UV exposures (cf. Fig. 5). In the case of beta irradiation, no decrease was observed, a result that is consistent with the linear increase of the TL main peak signal for longer UV exposures.

## 5. Conclusions

In this paper, the response of an  $\text{Al}_2\text{O}_3\text{:C,Mg}$  single crystal to UV irradiation was investigated by TL measurements. TL results showed three low-intensity peaks at about 320 K (peak I), 350 K (peak II) and 375 K (peak III), while the main peak (peak IV) was observed at 455 K. Comparison between UV and beta irradiations showed similar glow curves, although the TL mechanisms involved (release and trapping of charge carriers) are different. UV irradiation led to a saturating exponential response as a function of the irradiation exposure. Saturation was attributed to the unique characteristics of the absorption and dissipation of the incoming radiation, as well as changes in the F-type/F-aggregate concentrations.

## Declaration of competing interests

The authors declare that they have no known competing financial interests or personal relationships that could have appeared to influence the work reported in this paper.



## CRedit authorship contribution statement

**N.M. Trindade:** Conceptualization, Methodology, Validation, Writing - review & editing. **M.G. Magalhães:** Investigation, Formal analysis, Data curation. **M.C.S. Nunes:** Investigation, Data curation. **E. M. Yoshimura:** Resources, Supervision, Writing - review & editing. **L.G. Jacobsohn:** Resources, Supervision, Writing - review & editing.

## Acknowledgments

N. M. Trindade (#2019/05915–3); M. G. Magalhães (#2019/00942–2) and M. C. S. Nunes (#2018/16894–4) are grateful to São Paulo Research Foundation (FAPESP). E. M. Yoshimura thanks CNPq, grant #306843/2018–8. L. G. Jacobsohn is grateful to National Science Foundation, grant #1653016. The authors are grateful to Dr. M.S. Akselrod with Landauer, Inc., Crystal Growth Division, Stillwater, OK, for the  $\alpha$ -Al<sub>2</sub>O<sub>3</sub>:C,Mg crystal. In addition, the authors are grateful to L. S. Lima and L. Caldas for the help in the methodology of the measurements, as well as to E. G. Yukihiro for valuable discussions of the results.

## References

- [1] P. Vecchia, M. Hietanen, B.E. Stuck, E. van Deventer, S. Niu, Protecting Workers from Ultraviolet Radiation, Oberschleibheim, 2007.
- [2] C.M.H. Driscoll, Dosimetry methods for UV radiation, *Radiat. Protect. Dosim.* 72 (1997) 217–222.
- [3] V.H. Oliveira, Study of the luminescence of LaAlO<sub>3</sub> material doped with optically active trivalent ions for application in dosimetry of gamma and UV radiation, in: *Science and Technology of Radiation, Minerals and Materials*, Centro de Desenvolvimento da Tecnologia Nuclear (CDTN), Belo Horizonte, 2011, p. 80.
- [4] S.W.S. McKeever, *Thermoluminescence of Solids*, Cambridge University Press, Cambridge, 1985.
- [5] D.A. Sono, S.W.S. McKeever, Phototransferred thermoluminescence for use in UVB dosimetry, *Radiat. Protect. Dosim.* 100 (2002) 309–312.
- [6] L.E. Colyott, M.S. Akselrod, S.W.S. McKeever, Phototransferred thermoluminescence in alpha-Al<sub>2</sub>O<sub>3</sub>:C, radiation protection, *Dosimetry* 65 (1996) 263–266.
- [7] C. Cordoba, I. Aguirre de Carcer, F. Jaque, Behaviour of the a-Al<sub>2</sub>O<sub>3</sub>:C solar ultraviolet dosimeter under environmental conditions, *Radiat. Protect. Dosim.* 85 (1999) 321–324.
- [8] L. Oster, D. Weiss, N. Kristianpoller, A study of photostimulated thermoluminescence in C-doped alpha -Al<sub>2</sub>O<sub>3</sub>crystals, *J. Phys. Appl. Phys.* 27 (1994) 1732–1736.
- [9] A.S. Pradhan, P.K. Dash Sharma, V.K. Shirva, Thermoluminescence response of AL<sub>2</sub>O<sub>3</sub>:C to UV and ionising radiation, *Radiat. Protect. Dosim.* 64 (1996) 227–231.
- [10] R.P. Salas, R. Aceves, R. Meléndrez, M. Barboza-Flores, L.P. Pashchenko, Ultraviolet dosimetric properties of  $\alpha$ -Al<sub>2</sub>O<sub>3</sub> crystals, *Appl. Phys. Lett.* 63 (1993) 894–895.
- [11] E.G. Yukihiro, V.H. Whitley, J.C. Polf, D.M. Klein, S.W.S. McKeever, A.E. Akselrod, M.S. Akselrod, The effects of deep trap population on the thermoluminescence of Al<sub>2</sub>O<sub>3</sub>:C, *Radiat. Meas.* 37 (2003) 627–638.
- [12] V. Pagonis, R. Chen, J.L. Lawless, A quantitative kinetic model for Al<sub>2</sub>O<sub>3</sub>:C: TL response to UV-illumination, *Radiat. Meas.* 43 (2008) 175–179.
- [13] C.C. Gronchi, L.V.E. Caldas, PTOSL response of commercial Al<sub>2</sub>O<sub>3</sub>:C detectors to ultraviolet radiation, *Radiat. Protect. Dosim.* 154 (2013) 117–120.
- [14] J.M. Kalita, M.L. Chithambo, A comparative study of the dosimetric features of  $\alpha$ -Al<sub>2</sub>O<sub>3</sub>:C,Mg and  $\alpha$ -Al<sub>2</sub>O<sub>3</sub>:C, radiation protection, *Dosimetry* 177 (2017) 261–271.
- [15] E.G. Yukihiro, S.W.S. McKeever, Spectroscopy and optically stimulated luminescence of Al<sub>2</sub>O<sub>3</sub>:C using time-resolved measurements, *J. Appl. Phys.* 100 (2006), 083512.
- [16] J.M. Kalita, M.L. Chithambo, The influence of dose on the kinetic parameters and dosimetric features of the main thermoluminescence glow peak in  $\alpha$ -Al<sub>2</sub>O<sub>3</sub>:C,Mg, *Nucl. Instrum. Methods Phys. Res. Sect. B Beam Interact. Mater. Atoms* 394 (2017) 12–19.
- [17] M.S. Akselrod, A.E. Akselrod, S.S. Orlov, S. Sanyal, T.H. Underwood, New aluminum oxide single crystals for volumetric optical data storage, in: *Optical Data Storage*, Optical Society of America, Vancouver, 2003, p. TuC3.
- [18] J.M. Kalita, M.L. Chithambo, On the sensitivity of thermally and optically stimulated luminescence of  $\alpha$ -Al<sub>2</sub>O<sub>3</sub>:C and  $\alpha$ -Al<sub>2</sub>O<sub>3</sub>:C,Mg, *Radiat. Meas.* 99 (2017) 18–24.
- [19] M.S. Akselrod, A.E. Akselrod, New Al<sub>2</sub>O<sub>3</sub>:C,Mg crystals for radiophotoluminescent dosimetry and optical imaging, *Radiat. Protect. Dosim.* 119 (2006) 218–221.
- [20] G.M. Akselrod, M.S. Akselrod, E.R. Benton, N. Yasuda, A novel Al<sub>2</sub>O<sub>3</sub> fluorescent nuclear track detector for heavy charged particles and neutrons, *Nucl. Instrum. Methods Phys. Res. Sect. B Beam Interact. Mater. Atoms* 247 (2006) 295–306.
- [21] N.M. Trindade, L.G. Jacobsohn, Thermoluminescence and radioluminescence of  $\alpha$ -Al<sub>2</sub>O<sub>3</sub>:C,Mg at high temperatures, *J. Lumin.* 204 (2018) 598–602.
- [22] M.S. Akselrod, G.J. Sykora, Fluorescent nuclear track detector technology – a new way to do passive solid state dosimetry, *Radiat. Meas.* 46 (2011) 1671–1679.
- [23] S.A. Eller, M.F. Ahmed, J.A. Bartz, M.S. Akselrod, G. Denis, E.G. Yukihiro, Radiophotoluminescence properties of Al<sub>2</sub>O<sub>3</sub>:C,Mg crystals, *Radiat. Meas.* 56 (2013) 179–182.
- [24] G.J. Sykora, M.S. Akselrod, M. Salasky, S.A. Marino, Novel Al<sub>2</sub>O<sub>3</sub>:C,Mg fluorescent nuclear track detectors for passive neutron dosimetry, *Radiat. Protect. Dosim.* 126 (2007) 278–283.
- [25] G. Klimpki, J.M. Osinga, R. Herrmann, M.S. Akselrod, O. Jäkel, S. Greilich, Ion range measurements using fluorescent nuclear track detectors, *Radiat. Meas.* 56 (2013) 342–346.
- [26] G.J. Sykora, M.S. Akselrod, F. Vanhavere, Performance of fluorescence nuclear track detectors in mono-energetic and broad spectrum neutron fields, *Radiat. Meas.* 44 (2009) 988–991.
- [27] G.J. Sykora, M. Salasky, M.S. Akselrod, Properties of novel fluorescent nuclear track detectors for use in passive neutron dosimetry, *Radiat. Meas.* 43 (2008) 1017–1023.
- [28] M.S. Akselrod, Fundamentals of materials, techniques, and instrumentation for OSL and FNTD dosimetry, *AIP Conf. Proc.* 1345 (2011) 274–302.
- [29] N.M. Trindade, L.G. Jacobsohn, E.M. Yoshimura, Correlation between thermoluminescence and optically stimulated luminescence of  $\alpha$ -Al<sub>2</sub>O<sub>3</sub>:C,Mg, *J. Lumin.* 206 (2019) 298–301.
- [30] J.M. Kalita, M.L. Chithambo, Thermoluminescence of  $\alpha$ -Al<sub>2</sub>O<sub>3</sub>:C,Mg: kinetic analysis of the main glow peak, *J. Lumin.* 182 (2017) 177–182.
- [31] J.M. Kalita, M.L. Chithambo, The effect of annealing and beta irradiation on thermoluminescence spectra of  $\alpha$ -Al<sub>2</sub>O<sub>3</sub>:C,Mg, *J. Lumin.* 196 (2018) 195–200.
- [32] M. Puchalska, P. Bilski, GlowFit—a new tool for thermoluminescence glow-curve deconvolution, *Radiat. Meas.* 41 (2006) 659–664.
- [33] J.T. Randall, M.H.F. Wilkins, Phosphorescence and electron traps - I. The study of trap distributions, *Proc. Roy. Soc. Lond. Math. Phys. Sci.* 184 (1945) 365–389.
- [34] S. Sanyal, M.S. Akselrod, Anisotropy of optical absorption and fluorescence in Al<sub>2</sub>O<sub>3</sub>:C,Mg crystals, *J. Appl. Phys.* 98 (2005), 033518.
- [35] B.D. Evans, G.J. Pogatschnik, Y. Chen, Optical properties of lattice defects in  $\alpha$ -Al<sub>2</sub>O<sub>3</sub>, *Nucl. Instrum. Methods Phys. Res. Sect. B Beam Interact. Mater. Atoms* 91 (1994) 258–262.
- [36] G.J. Sykora, M.S. Akselrod, Photoluminescence study of photochromically and radiochromically transformed Al<sub>2</sub>O<sub>3</sub>:C,Mg crystals used for fluorescent nuclear track detectors, *Radiat. Meas.* 45 (2010) 631–634.
- [37] E.W.J. Mitchell, J.D. Rigden, P.D. Townsend, The anisotropy of optical absorption induced in sapphire by neutron and electron irradiation, *Phil. Mag.: J. Theoretical Exp. Appl. Phys.* 5 (1960) 1013–1027.
- [38] M.G. Rodriguez, G. Denis, M.S. Akselrod, T.H. Underwood, E.G. Yukihiro, Thermoluminescence, optically stimulated luminescence and radioluminescence properties of Al<sub>2</sub>O<sub>3</sub>:C,Mg, *Radiat. Meas.* 46 (2011) 1469–1473.
- [39] J.M. Kalita, M.L. Chithambo, Comprehensive kinetic analysis of thermoluminescence peaks of  $\alpha$ -Al<sub>2</sub>O<sub>3</sub>:C,Mg, *J. Lumin.* 185 (2017) 72–82.
- [40] A. Morono, E.R. Hodgson, On the origin of the F+ centre radioluminescence in sapphire, *J. Nucl. Mater.* 249 (1997) 128–132.
- [41] I.I. Mil'man, E.V. Moiseikin, S.V. Nikiforov, S.V. Solov'ev, I.G. Revkov, E. N. Litovchenko, The role of deep traps in luminescence of anion-defective  $\alpha$ -Al<sub>2</sub>O<sub>3</sub>:C crystals, *Phys. Solid State* 50 (2008) 2076–2080.